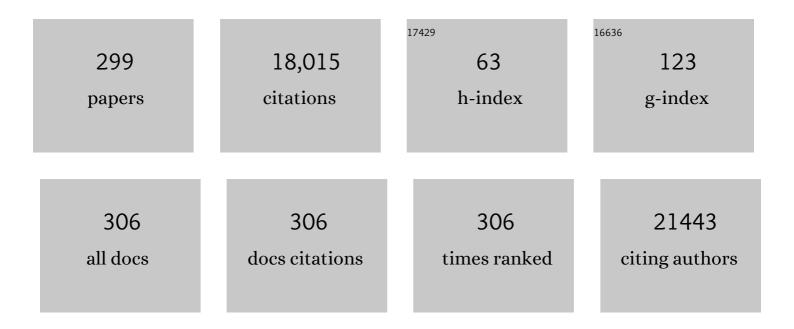
## Xi-Wen Du

List of Publications by Year in descending order

Source: https://exaly.com/author-pdf/3741567/publications.pdf Version: 2024-02-01



#	Article	IF	CITATIONS
1	Porous P-doped graphitic carbon nitride nanosheets for synergistically enhanced visible-light photocatalytic H <sub>2</sub> production. Energy and Environmental Science, 2015, 8, 3708-3717.	15.6	1,146
2	One-step synthesis of fluorescent carbon nanoparticles by laser irradiation. Journal of Materials Chemistry, 2009, 19, 484-488.	6.7	829
3	Nanomaterials via Laser Ablation/Irradiation in Liquid: A Review. Advanced Functional Materials, 2012, 22, 1333-1353.	7.8	775
4	Superhydrophobic Surfaces: Are They Really Ice-Repellent?. Langmuir, 2011, 27, 25-29.	1.6	592
5	Engineering surface atomic structure of single-crystal cobalt (II) oxide nanorods for superior electrocatalysis. Nature Communications, 2016, 7, 12876.	5.8	568
6	Engineering oxygen vacancy on NiO nanorod arrays for alkaline hydrogen evolution. Nano Energy, 2018, 43, 103-109.	8.2	515
7	Theory-driven design of high-valence metal sites for water oxidation confirmed using in situ soft X-ray absorption. Nature Chemistry, 2018, 10, 149-154.	6.6	476
8	Identifying the Key Role of Pyridinicâ€N–Co Bonding in Synergistic Electrocatalysis for Reversible ORR/OER. Advanced Materials, 2018, 30, e1800005.	11.1	394
9	Sulfur-Modulated Tin Sites Enable Highly Selective Electrochemical Reduction of CO2 to Formate. Joule, 2017, 1, 794-805.	11.7	390
10	Nâ€Đoped Graphene Natively Grown on Hierarchical Ordered Porous Carbon for Enhanced Oxygen Reduction. Advanced Materials, 2013, 25, 6226-6231.	11.1	388
11	Activating cobalt(II) oxide nanorods for efficient electrocatalysis by strain engineering. Nature Communications, 2017, 8, 1509.	5.8	361
12	An Approach to Obtaining Homogeneously Dispersed Carbon Nanotubes in Al Powders for Preparing Reinforced Al-Matrix Composites. Advanced Materials, 2007, 19, 1128-1132.	11.1	321
13	Rutheniumâ€Based Singleâ€Atom Alloy with High Electrocatalytic Activity for Hydrogen Evolution. Advanced Energy Materials, 2019, 9, 1803913.	10.2	270
14	Engineering NiO/NiFe LDH Intersection to Bypass Scaling Relationship for Oxygen Evolution Reaction via Dynamic Tridimensional Adsorption of Intermediates. Advanced Materials, 2019, 31, e1804769.	11.1	264
15	Stable Aqueous Dispersion of ZnO Quantum Dots with Strong Blue Emission via Simple Solution Route. Journal of the American Chemical Society, 2007, 129, 16029-16033.	6.6	261
16	A silver catalyst activated by stacking faults for the hydrogen evolution reaction. Nature Catalysis, 2019, 2, 1107-1114.	16.1	245
17	Atomically and Electronically Coupled Pt and CoO Hybrid Nanocatalysts for Enhanced Electrocatalytic Performance. Advanced Materials, 2017, 29, 1604607.	11.1	224
18	Wellâ€Dispersed Nickel―and Zincâ€Tailored Electronic Structure of a Transition Metal Oxide for Highly Active Alkaline Hydrogen Evolution Reaction. Advanced Materials, 2019, 31, e1807771.	11.1	216

#	Article	IF	CITATIONS
19	Phase segregation reversibility in mixed-metal hydroxide water oxidation catalysts. Nature Catalysis, 2020, 3, 743-753.	16.1	199
20	Fully Oxidized Ni–Fe Layered Double Hydroxide with 100% Exposed Active Sites for Catalyzing Oxygen Evolution Reaction. ACS Catalysis, 2019, 9, 6027-6032.	5.5	165
21	Atomic-level structure engineering of metal oxides for high-rate oxygen intercalation pseudocapacitance. Science Advances, 2018, 4, eaau6261.	4.7	164
22	Copper adparticle enabled selective electrosynthesis of n-propanol. Nature Communications, 2018, 9, 4614.	5.8	153
23	Highly ordered mesoporous Cr <sub>2</sub> O <sub>3</sub> materials with enhanced performance for gas sensors and lithium ion batteries. Chemical Communications, 2012, 48, 865-867.	2.2	152
24	Ir–O–V Catalytic Group in Ir-Doped NiV(OH) <sub>2</sub> for Overall Water Splitting. ACS Energy Letters, 2019, 4, 1823-1829.	8.8	147
25	Morphology Control of Nanostructures via Surface Reaction of Metal Nanodroplets. Journal of the American Chemical Society, 2010, 132, 9814-9819.	6.6	140
26	Progress and Challenges Toward the Rational Design of Oxygen Electrocatalysts Based on a Descriptor Approach. Advanced Science, 2020, 7, 1901614.	5.6	133
27	Multiscale Structural Engineering of Niâ€Doped CoO Nanosheets for Zinc–Air Batteries with High Power Density. Advanced Materials, 2018, 30, e1804653.	11.1	131
28	Charge distribution guided by grain crystallographic orientations in polycrystalline battery materials. Nature Communications, 2020, 11, 83.	5.8	129
29	Hollow Nanoparticles of Metal Oxides and Sulfides: Fast Preparation via Laser Ablation in Liquid. Langmuir, 2010, 26, 16652-16657.	1.6	118
30	Stable Rhodium (IV) Oxide for Alkaline Hydrogen Evolution Reaction. Advanced Materials, 2020, 32, e1908521.	11.1	115
31	Laser-Prepared CuZn Alloy Catalyst for Selective Electrochemical Reduction of CO <sub>2</sub> to Ethylene. Langmuir, 2018, 34, 13544-13549.	1.6	114
32	Top-Down Preparation of Active Cobalt Oxide Catalyst. ACS Catalysis, 2016, 6, 6699-6703.	5.5	113
33	Deciphering the Cathode–Electrolyte Interfacial Chemistry in Sodium Layered Cathode Materials. Advanced Energy Materials, 2018, 8, 1801975.	10.2	111
34	Laser synthesis of oxygen vacancy-modified CoOOH for highly efficient oxygen evolution. Chemical Communications, 2019, 55, 2904-2907.	2.2	110
35	Co <sub>3</sub> O <sub>4</sub> Nanoparticles with Ultrasmall Size and Abundant Oxygen Vacancies for Boosting Oxygen Involved Reactions. Advanced Functional Materials, 2019, 29, 1903444.	7.8	108
36	A top–down strategy towards monodisperse colloidal lead sulphide quantum dots. Nature Communications, 2013, 4, 1695.	5.8	106

#	Article	IF	CITATIONS
37	Freestanding Ultrathin Metallic Nanosheets: Materials, Synthesis, and Applications. Advanced Materials, 2015, 27, 5396-5402.	11.1	102
38	The icephobic performance of alkyl-grafted aluminum surfaces. Soft Matter, 2015, 11, 856-861.	1.2	101
39	Properties of Coreâ ''Shell Niâ ''Au Nanoparticles Synthesized through a Redox-Transmetalation Method in Reverse Microemulsion. Chemistry of Materials, 2007, 19, 3399-3405.	3.2	100
40	Engineering hierarchical nanotrees with CuCo <sub>2</sub> O <sub>4</sub> trunks and NiO branches for high-performance supercapacitors. Journal of Materials Chemistry A, 2017, 5, 5820-5828.	5.2	100
41	Synthesis of Palladiumâ€Based Crystalline@Amorphous Core–Shell Nanoplates for Highly Efficient Ethanol Oxidation. Advanced Materials, 2020, 32, e2000482.	11.1	98
42	Revealing the Dynamics and Roles of Iron Incorporation in Nickel Hydroxide Water Oxidation Catalysts. Journal of the American Chemical Society, 2021, 143, 18519-18526.	6.6	96
43	Strongly Coupled Nafion Molecules and Ordered Porous CdS Networks for Enhanced Visibleâ€Light Photoelectrochemical Hydrogen Evolution. Advanced Materials, 2016, 28, 4935-4942.	11.1	95
44	Synthesis of hollow carbon nano-onions and their use for electrochemical hydrogen storage. Carbon, 2012, 50, 3513-3521.	5.4	94
45	Strongly Coupled CoO Nanoclusters/CoFe LDHs Hybrid as a Synergistic Catalyst for Electrochemical Water Oxidation. Small, 2018, 14, e1800195.	5.2	91
46	Ti3+ defect mediated g-C3N4/TiO2 Z-scheme system for enhanced photocatalytic redox performance. Applied Surface Science, 2018, 448, 288-296.	3.1	89
47	Operando Revealing Dynamic Reconstruction of NiCo Carbonate Hydroxide for High-Rate Energy Storage. Joule, 2020, 4, 673-687.	11.7	88
48	Formation of crystalline Si nanodots in SiO2 films by electron irradiation. Applied Physics Letters, 2003, 82, 1108-1110.	1.5	83
49	Zinc-Blende CdS Nanocubes with Coordinated Facets for Photocatalytic Water Splitting. ACS Catalysis, 2017, 7, 1470-1477.	5.5	83
50	A novel method for making open cell aluminum foams by powder sintering process. Materials Letters, 2005, 59, 3333-3336.	1.3	80
51	Bionic Design of a Mo(IV)-Doped FeS <sub>2</sub> Catalyst for Electroreduction of Dinitrogen to Ammonia. ACS Catalysis, 2020, 10, 4914-4921.	5.5	80
52	Silver/Copper Interface for Relay Electroreduction of Carbon Dioxide to Ethylene. ACS Applied Materials & amp; Interfaces, 2019, 11, 2763-2767.	4.0	77
53	Complete UV emission of ZnO nanoparticles in a PMMA matrix. Semiconductor Science and Technology, 2006, 21, 1202-1206.	1.0	74
54	Low-temperature CVD synthesis of carbon-encapsulated magnetic Ni nanoparticles with a narrow distribution of diameters. Carbon, 2006, 44, 2330-2333.	5.4	74

#	Article	IF	CITATIONS
55	ZnS/ZnO Heteronanostructure as Photoanode to Enhance the Conversion Efficiency of Dye-Sensitized Solar Cells. Journal of Physical Chemistry C, 2010, 114, 2380-2384.	1.5	74
56	Enhanced multi-carbon alcohol electroproduction from CO via modulated hydrogen adsorption. Nature Communications, 2020, 11, 3685.	5.8	72
57	Modest Oxygenâ€Defective Amorphous Manganeseâ€Based Nanoparticle Mullite with Superior Overall Electrocatalytic Performance for Oxygen Reduction Reaction. Small, 2017, 13, 1603903.	5.2	69
58	Iridium Oxide Modified with Silver Single Atom for Boosting Oxygen Evolution Reaction in Acidic Media. ACS Energy Letters, 0, , 1588-1595.	8.8	69
59	Electrocatalytic Reduction of Low-Concentration Nitric Oxide into Ammonia over Ru Nanosheets. ACS Energy Letters, 2022, 7, 1187-1194.	8.8	68
60	Gas-Phase Cation Exchange toward Porous Single-Crystal CoO Nanorods for Catalytic Hydrogen Production. Chemistry of Materials, 2015, 27, 352-357.	3.2	67
61	Ionic liquid-assisted synthesis of N/S-double doped graphene microwires for oxygen evolution and Zn–air batteries. Energy Storage Materials, 2015, 1, 17-24.	9.5	67
62	Tuning the selectivity and activity of Au catalysts for carbon dioxide electroreduction via grain boundary engineering: a DFT study. Journal of Materials Chemistry A, 2017, 5, 7184-7190.	5.2	66
63	Carbon nanotubes and onions from methane decomposition using Ni/Al catalysts. Materials Chemistry and Physics, 2006, 97, 109-115.	2.0	65
64	Interrogation of bimetallic particle oxidation in three dimensions at the nanoscale. Nature Communications, 2016, 7, 13335.	5.8	65
65	Control of Cu-doping and optical properties of ZnO quantum dots by laser ablation of composite targets. Materials Chemistry and Physics, 2011, 130, 425-430.	2.0	64
66	Surface plasmon resonance enhanced visible-light-driven photocatalytic activity in Cu nanoparticles covered Cu2O microspheres for degrading organic pollutants. Applied Surface Science, 2016, 366, 120-128.	3.1	64
67	Zn nanosheets coated with a ZnS subnanometer layer for effective and durable CO <sub>2</sub> reduction. Journal of Materials Chemistry A, 2019, 7, 1418-1423.	5.2	63
68	The efficient synthesis of carbon nano-onions using chemical vapor deposition on an unsupported Ni–Fe alloy catalyst. Carbon, 2011, 49, 1151-1158.	5.4	62
69	Ultrafine diamond synthesized by long-pulse-width laser. Applied Physics Letters, 2006, 89, 183115.	1.5	60
70	Enhanced electrochemical hydrogen storage capacity of multi-walled carbon nanotubes by TiO2 decoration. International Journal of Hydrogen Energy, 2011, 36, 6739-6743.	3.8	60
71	Low-temperature synthesis of carbon onions by chemical vapor deposition using a nickel catalyst supported on aluminum. Scripta Materialia, 2006, 54, 689-693.	2.6	59
72	ZnO nanosheets with atomically thin ZnS overlayers for photocatalytic water splitting. Journal of Materials Chemistry A, 2018, 6, 9057-9063.	5.2	59

#	Article	IF	CITATIONS
73	Pyrite nanorod arrays as an efficient counter electrode for dye-sensitized solar cells. Journal of Materials Chemistry A, 2013, 1, 11828.	5.2	58
74	Laser synthesis of gold/oxide nanocomposites. Journal of Materials Chemistry, 2010, 20, 1103-1106.	6.7	57
75	Enhanced electrochemical performance of LiFePO4 cathode with in-situ chemical vapor deposition synthesized carbon nanotubes as conductor. Journal of Power Sources, 2012, 220, 264-268.	4.0	57
76	Galvanic Replacement Reactions of Activeâ€Metal Nanoparticles. Chemistry - A European Journal, 2012, 18, 4234-4241.	1.7	56
77	ZnFe <sub>2</sub> O <sub>4</sub> Leaves Grown on TiO <sub>2</sub> Trees Enhance Photoelectrochemical Water Splitting. Small, 2016, 12, 3181-3188.	5.2	56
78	3D Aluminum Hybrid Plasmonic Nanostructures with Large Areas of Dense Hot Spots and Longâ€Term Stability. Advanced Functional Materials, 2017, 27, 1605703.	7.8	56
79	The formation of multiply twinning structure and photoluminescence of well-dispersed nanodiamonds produced by pulsed-laser irradiation. Diamond and Related Materials, 2008, 17, 142-146.	1.8	55
80	Scalable synthesis of hollow Cu <sub>2</sub> O nanocubes with unique optical properties via a simple hydrolysis-based approach. Journal of Materials Chemistry A, 2013, 1, 302-307.	5.2	55
81	Catalytically active and chemically inert CdIn <sub>2</sub> S <sub>4</sub> coating on a CdS photoanode for efficient and stable water splitting. Nanoscale, 2017, 9, 6296-6301.	2.8	55
82	Laser-Generated Grain Boundaries in Ruthenium Nanoparticles for Boosting Oxygen Evolution Reaction. ACS Catalysis, 2020, 10, 12575-12581.	5.5	55
83	A Hydrogenâ€Deficient Nickel–Cobalt Double Hydroxide for Photocatalytic Overall Water Splitting. Angewandte Chemie - International Edition, 2020, 59, 11510-11515.	7.2	55
84	Thermogravimetric analysis and TEM characterization of the oxidation and defect sites of carbon nanotubes synthesized by CVD of methane. Materials Science & Engineering A: Structural Materials: Properties, Microstructure and Processing, 2008, 473, 355-359.	2.6	54
85	A One-compartment direct glucose alkaline fuel cell with methyl viologen as electron mediator. Applied Energy, 2013, 106, 176-183.	5.1	54
86	Single crystalline Cu <sub>2</sub> ZnSnS <sub>4</sub> nanosheet arrays for efficient photochemical hydrogen generation. RSC Advances, 2015, 5, 2543-2549.	1.7	53
87	Molybdenum Disulfide Modified by Laser Irradiation for Catalyzing Hydrogen Evolution. ACS Sustainable Chemistry and Engineering, 2019, 7, 6999-7003.	3.2	53
88	Direct synthesis of SiC nanowires by multiple reaction VS growth. Materials Science and Engineering B: Solid-State Materials for Advanced Technology, 2007, 136, 72-77.	1.7	51
89	Synthesis and characterization of Ag nanoparticles assembled in ordered array pores of porous anodic alumina by chemical deposition. Materials Letters, 2007, 61, 3795-3797.	1.3	50
90	Effects of anodizing conditions on anodic alumina structure. Journal of Materials Science, 2007, 42, 3878-3882.	1.7	50

#	Article	IF	CITATIONS
91	Synthesis and Sensing Properties of ZnO/ZnS Nanocages. Nanoscale Research Letters, 2010, 5, 644-648.	3.1	48
92	Localized Defects on Copper Sulfide Surface for Enhanced Plasmon Resonance and Water Splitting. Small, 2017, 13, 1700867.	5.2	48
93	Tuning Spin State of Rockâ€Saltâ€Based Oxides by Manipulation of Crystallinity for Efficient Oxygen Electrocatalysis. Advanced Energy Materials, 2018, 8, 1703469.	10.2	48
94	Creating compressive stress at the NiOOH/NiO interface for water oxidation. Journal of Materials Chemistry A, 2020, 8, 10747-10754.	5.2	47
95	Porous Cobalt–Nickel Hydroxide Nanosheets with Active Cobalt Ions for Overall Water Splitting. Small, 2019, 15, e1804832.	5.2	46
96	Strainâ€Activated Copper Catalyst for pHâ€Universal Hydrogen Evolution Reaction. Advanced Functional Materials, 2022, 32, .	7.8	46
97	NiO nanotubes assembled in pores of porous anodic alumina and their optical absorption properties. Chemical Physics Letters, 2008, 454, 75-79.	1.2	44
98	Laser Dispersion of Detonation Nanodiamonds. Angewandte Chemie - International Edition, 2011, 50, 4099-4102.	7.2	44
99	Comparison of ZnO and TiO2 nanowires for photoanode of dye-sensitized solar cells. Journal of Alloys and Compounds, 2013, 546, 307-313.	2.8	44
100	Identifying the descriptor governing NO oxidation on mullite Sm(Y, Tb, Gd,) Tj ETQq0 0 0 rgBT /Overlock 10 Tf 5 2016, 6, 3971-3975.	0 387 Td ( 2.1	Lu)Mn <sub> 44</sub>
101	Hierarchical porous carbon with graphitic structure synthesized by a water soluble template method. Materials Letters, 2012, 87, 77-79.	1.3	43
102	Synthesis of carbon nanotubes and carbon onions by CVD using a Ni/Y catalyst supported on copper. Materials Science & Engineering A: Structural Materials: Properties, Microstructure and Processing, 2008, 475, 136-140.	2.6	42
103	Cuprous ions embedded in ceria lattice for selective and stable electrochemical reduction of carbon dioxide to ethylene. Journal of Materials Chemistry A, 2018, 6, 9373-9377.	5.2	42
104	Laser-induced oxygen vacancies in FeCo <sub>2</sub> O <sub>4</sub> nanoparticles for boosting oxygen evolution and reduction. Chemical Communications, 2019, 55, 8579-8582.	2.2	41
105	Unveiling the critical role of the Mn dopant in a NiFe(OH) <sub>2</sub> catalyst for water oxidation. Journal of Materials Chemistry A, 2020, 8, 17471-17476.	5.2	41
106	In situ formation of Cu–ZrO2 composites by chemical routes. Journal of Alloys and Compounds, 2006, 425, 390-394.	2.8	40
107	CdS Nanoflake Arrays for Highly Efficient Light Trapping. Advanced Materials, 2015, 27, 740-745.	11.1	40
108	Nanometre Ni and core/shell Ni/Au nanoparticles with controllable dimensions synthesized in reverse microemulsion. Journal of Alloys and Compounds, 2009, 475, 494-500.	2.8	39

#	Article	IF	CITATIONS
109	High-performance glucose fuel cell with bimetallic Ni–Co composite anchored on reduced graphene oxide as anode catalyst. Renewable Energy, 2020, 155, 1118-1126.	4.3	39
110	Arrays of Ultrathin CdS Nanoflakes with High-Energy Surface for Efficient Gas Detection. ACS Applied Materials & Interfaces, 2017, 9, 602-609.	4.0	38
111	Thermally driven mesoscale chemomechanical interplay in Li <sub>0.5</sub> Ni <sub>0.6</sub> Mn <sub>0.2</sub> Co <sub>0.2</sub> O <sub>2</sub> cathode materials. Journal of Materials Chemistry A, 2018, 6, 23055-23061.	5.2	38
112	Lattice-strained palladium nanoparticles as active catalysts for the oxygen reduction reaction. Chemical Communications, 2019, 55, 3121-3123.	2.2	38
113	Strawberry-like Co3O4-Ag bifunctional catalyst for overall water splitting. Applied Catalysis B: Environmental, 2021, 299, 120658.	10.8	38
114	A practical method for the production of hollow carbon onion particles. Journal of Alloys and Compounds, 2006, 425, 329-333.	2.8	37
115	Synthesis and growth mechanism of metal filled carbon nanostructures by CVD using Ni/Y catalyst supported on copper. Journal of Alloys and Compounds, 2008, 456, 290-296.	2.8	36
116	Improved visible photoluminescence from porous silicon with surface Si–Ag bonds. Applied Physics Letters, 2005, 86, 171905.	1.5	35
117	Effects of alloying elements on creep of TiAl alloys with a fine lamellar structure. Acta Materialia, 2002, 50, 1307-1318.	3.8	34
118	Effect of Y2O3 on the mechanical properties of open cell aluminum foams. Materials Letters, 2006, 60, 1665-1668.	1.3	34
119	Highly Conductive CdS Inverse Opals for Photochemical Solar Cells. Advanced Functional Materials, 2014, 24, 707-715.	7.8	34
120	Bond-Energy-Integrated Descriptor for Oxygen Electrocatalysis of Transition Metal Oxides. Journal of Physical Chemistry Letters, 2018, 9, 3387-3391.	2.1	34
121	The influences of synthesis temperature and Ni catalyst on the growth of carbon nanotubes by chemical vapor deposition. Materials Letters, 2008, 62, 1472-1475.	1.3	33
122	An Ordered P2/P3 Composite Layered Oxide Cathode with Long Cycle Life in Sodium-Ion Batteries. , 2019, 1, 573-581.		33
123	Electroreduction of Carbon Dioxide in Metallic Nanopores through a Pincer Mechanism. Angewandte Chemie - International Edition, 2020, 59, 19297-19303.	7.2	33
124	Influence of surface Si–Ag bonds on photoluminescence of porous silicon. Journal of Applied Physics, 2006, 100, 063512.	1.1	32
125	Intensive light emission from SiCN films by reactive RF magnetron sputtering. Materials Chemistry and Physics, 2007, 103, 456-460.	2.0	32
126	Fabrication and properties of carbon nanotubes reinforced Fe/hydroxyapatite composites by in situ chemical vapor deposition. Composites Part A: Applied Science and Manufacturing, 2008, 39, 1128-1132.	3.8	32

#	Article	IF	CITATIONS
127	Fabrication of aluminum matrix composites with enhanced mechanical properties reinforced by in situ generated MgAl2O4 whiskers. Composites Part A: Applied Science and Manufacturing, 2012, 43, 631-634.	3.8	31
128	A stable inverse opal structure of cadmium chalcogenide for efficient water splitting. Journal of Materials Chemistry A, 2015, 3, 18521-18527.	5.2	31
129	Valence‧tate Effect of Iridium Dopant in NiFe(OH) <sub>2</sub> Catalyst for Hydrogen Evolution Reaction. Small, 2021, 17, e2100203.	5.2	31
130	Synthesis of carbon nanostructures with different morphologies by CVD of methane. Materials Science & Engineering A: Structural Materials: Properties, Microstructure and Processing, 2007, 460-461, 255-260.	2.6	30
131	The effect of post-annealing on the conversion efficiency of solar cells sensitized by CdS quantum dots. Semiconductor Science and Technology, 2010, 25, 045031.	1.0	30
132	P-type CoO nanowire arrays and their application in quantum dot-sensitized solar cells. RSC Advances, 2013, 3, 1217-1221.	1.7	30
133	Facile synthesis of three dimensional CdS nanoflowers with high photocatalytic performance. Journal of Alloys and Compounds, 2016, 656, 972-977.	2.8	30
134	Improving Interfacial Electron Transfer via Tuning Work Function of Electrodes for Electrocatalysis: From Theory to Experiment. Journal of Physical Chemistry C, 2019, 123, 28319-28326.	1.5	30
135	Sulfateâ€Enabled Nitrate Synthesis from Nitrogen Electrooxidation on a Rhodium Electrocatalyst. Angewandte Chemie - International Edition, 2022, 61, .	7.2	30
136	Low-temperature synthesis of ZnO/CdS hierarchical nanostructure for photovoltaic application. Nanoscale, 2012, 4, 5602.	2.8	29
137	Microstructure and properties of in situ generated MgAl2O4 spinel whisker reinforced aluminum matrix composites. Materials & Design, 2013, 46, 724-730.	5.1	29
138	Photochemical Synthesis of Ultrafine Cubic Boron Nitride Nanoparticles under Ambient Conditions. Angewandte Chemie - International Edition, 2015, 54, 7051-7054.	7.2	29
139	Face-centered-cubic Si nanocrystals prepared by microsecond pulsed laser ablation. Journal of Applied Physics, 2007, 102, .	1.1	28
140	Fabrication and growth mechanism of Ni-filled carbon nanotubes by the catalytic method. Journal of Alloys and Compounds, 2008, 465, 51-55.	2.8	28
141	On the origin of blue emission from ZnO quantum dots synthesized by a sol–gel route. Semiconductor Science and Technology, 2012, 27, 065020.	1.0	28
142	Surface transformation by a "cocktail―solvent enables stable cathode materials for sodium ion batteries. Journal of Materials Chemistry A, 2018, 6, 2758-2766.	5.2	28
143	Selective nitrogen doping of graphene oxide by laser irradiation for enhanced hydrogen evolution activity. Chemical Communications, 2018, 54, 13726-13729.	2.2	28
144	Conductive Boron Nitride as Promising Catalyst Support for the Oxygen Evolution Reaction. Advanced Energy Materials, 2020, 10, 1902521.	10.2	28

#	Article	IF	CITATIONS
145	Fabrication of carbon-coated cobalt nanoparticles by the catalytic method. Journal of Alloys and Compounds, 2008, 458, 130-133.	2.8	27
146	ZnO hierarchical nanostructures and application on high-efficiency dye-sensitized solar cells. Materials Science and Engineering B: Solid-State Materials for Advanced Technology, 2010, 166, 196-202.	1.7	27
147	Microstructural characterization of creep cavitation in a fully-lamellar TiAl alloy. Intermetallics, 2001, 9, 137-146.	1.8	24
148	Spongy structure of CdS nanocrystals decorated with dye molecules for semiconductor sensitized solar cells. Journal of Materials Chemistry, 2011, 21, 2883.	6.7	24
149	Ultrafine SmMn2O5-Î <sup>^</sup> electrocatalysts with modest oxygen deficiency for highly-efficient pH-neutral magnesium-air batteries. Journal of Power Sources, 2020, 449, 227482.	4.0	24
150	Creep induced α2→β2phase transformation in a fully-lamellar TiAl alloy. Scripta Materialia, 2000, 43, 597-602.	2.6	23
151	Reinforcing copper matrix composites through molecular-level mixing of functionalized nanodiamond by co-deposition route. Materials Science & Engineering A: Structural Materials: Properties, Microstructure and Processing, 2008, 490, 293-299.	2.6	23
152	One-step synthesis of MgO hollow nanospheres with blue emission. Nanotechnology, 2010, 21, 295604.	1.3	23
153	Improve photo-electron conversion efficiency of ZnO/CdS coaxial nanorods by p-type CdTe coating. Nanotechnology, 2012, 23, 485401.	1.3	23
154	Laser synthesis of clean mesocrystal of cupric oxide for efficient gas sensing. Journal of Materials Chemistry A, 2016, 4, 2699-2704.	5.2	23
155	Porous Copper Microspheres for Selective Production of Multicarbon Fuels via CO <sub>2</sub> Electroreduction. Small, 2019, 15, e1902582.	5.2	23
156	Surface Valence State Effect of MoO <sub>2+</sub> <i><sub>x</sub></i> on Electrochemical Nitrogen Reduction. Advanced Science, 2022, 9, e2104857.	5.6	23
157	The evolution of microstructure and photoluminescence of SiCN films with annealing temperature. Journal of Applied Physics, 2006, 99, 093503.	1.1	22
158	Amorphous carbon nanotubes fabricated by low-temperature chemical vapor deposition. Carbon, 2006, 44, 1859-1862.	5.4	22
159	Single-crystal ZnO flocky sphere formed by three-dimensional oriented attachment of nanoparticles. Journal of Physics and Chemistry of Solids, 2008, 69, 880-883.	1.9	22
160	Boosting reversible oxygen electrocatalysis with enhanced interfacial pyridinic-N–Co bonding in cobalt oxide/mesoporous N-doped graphene hybrids. Nanoscale, 2018, 10, 22140-22147.	2.8	22
161	Water-Processable P2-Na <sub>0.67</sub> Ni <sub>0.22</sub> Cu <sub>0.11</sub> Mn <sub>0.56</sub> Ti <sub>0.11</sub> O <sub Material for Sodium Ion Batteries. Journal of the Electrochemical Society, 2019, 166, A251-A257.</sub 	>2< <b>⊈s</b> ub>C	Cathzzde
162	Single-Crystal ZnO Cup Based on Hydrothermal Decomposition Route. Journal of Physical Chemistry C, 2007, 111, 3863-3867.	1.5	21

#	Article	IF	CITATIONS
163	Controlling surface states and photoluminescence of porous silicon by low-energy-ion irradiation. Applied Surface Science, 2008, 254, 2479-2482.	3.1	21
164	Improving charge separation of solar cells by the co-sensitization of CdS quantum dots and dye. Semiconductor Science and Technology, 2010, 25, 095014.	1.0	21
165	Low-temperature synthesis of aluminum borate nanowhiskers on the surface of aluminum powder promoted by ball-milling pretreatment. Powder Technology, 2011, 212, 310-315.	2.1	21
166	Ultrafine Ag Nanoparticles as Active Catalyst for Electrocatalytic Hydrogen Production. ChemCatChem, 2019, 11, 5976-5981.	1.8	21
167	Preparation and photocatalytic properties of mixed-phase titania nanospheres by laser ablation. Materials Letters, 2009, 63, 2384-2386.	1.3	20
168	Double Open-Circuit Voltage of Three-Dimensional ZnO/CdTe Solar Cells by a Balancing Depletion Layer. ACS Applied Materials & amp; Interfaces, 2014, 6, 14718-14723.	4.0	20
169	Chlorella-derived porous heteroatom-doped carbons as robust catalysts for oxygen reduction reaction in direct glucose alkaline fuel cell. International Journal of Hydrogen Energy, 2019, 44, 2823-2831.	3.8	20
170	Formation and luminescent properties of face-centered-cubic Si nanocrystals in silica matrix by magnetron sputtering with substrate bias. Applied Physics Letters, 2007, 90, 241910.	1.5	19
171	Template synthesis and photovoltaic application of CdS nanotube arrays. Semiconductor Science and Technology, 2012, 27, 055017.	1.0	19
172	Superior gas-sensing performance of amorphous CdO nanoflake arrays prepared at room temperature. Journal of Materials Chemistry A, 2016, 4, 8700-8706.	5.2	19
173	Laser Synthesis of Iridium Nanospheres for Overall Water Splitting. Materials, 2019, 12, 3028.	1.3	19
174	Synthesis of binary and triple carbon nanotubes over Ni/Cu/Al2O3 catalyst by chemical vapor deposition. Materials Letters, 2007, 61, 4940-4943.	1.3	18
175	Enhancing the Conversion Efficiency of Semiconductor Sensitized Solar Cells via the Cosensitization of Dual-Sized Quantum Dots. Industrial & amp; Engineering Chemistry Research, 2012, 51, 10074-10078.	1.8	18
176	In-situ processing and aging behaviors of MgAl2O4 spinel whisker reinforced 6061Al composite. Materials Science & Engineering A: Structural Materials: Properties, Microstructure and Processing, 2014, 598, 114-121.	2.6	18
177	Millisecond Laser Ablation of Molybdenum Target in Reactive Gas toward MoS <sub>2</sub> Fullerene-Like Nanoparticles with Thermally Stable Photoresponse. ACS Applied Materials & Interfaces, 2015, 7, 1949-1954.	4.0	18
178	Laserâ€Ablationâ€Produced Cobalt Nickel Phosphate with Highâ€Valence Nickel Ions as an Active Catalyst for the Oxygen Evolution Reaction. Chemistry - A European Journal, 2020, 26, 2793-2797.	1.7	18
179	Engineering a Cu/ZnO <i><sub>x</sub></i> Interface for High Methane Selectivity in CO <sub>2</sub> Electrochemical Reduction. Industrial & Engineering Chemistry Research, 2021, 60, 273-280.	1.8	18
180	Study of aluminum powder as transition metal catalyst carrier for CVD synthesis of carbon nanotubes. Materials Science & Engineering A: Structural Materials: Properties, Microstructure and Processing, 2006, 441, 266-270.	2.6	17

#	Article	IF	CITATIONS
181	TEM investigation on the initial stage growth of carbon onions synthesized by CVD. Journal of Alloys and Compounds, 2008, 452, 258-262.	2.8	17
182	Facile synthesis of SnS hollow nanoparticles via laser ablation followed by chemical etching. RSC Advances, 2012, 2, 7824.	1.7	17
183	Direct Conversion of Bulk Metals to Sizeâ€Tailored, Monodisperse Spherical Nonâ€Coinageâ€Metal Nanocrystals. Angewandte Chemie - International Edition, 2015, 54, 4787-4791.	7.2	17
184	Formation of the creep-induced β2 phase and its influence on deformation in a fully-lamellar TiAl alloy. Intermetallics, 2001, 9, 181-187.	1.8	16
185	Structure evolution of silicon nanocrystals under electron irradiation. Scripta Materialia, 2005, 53, 899-903.	2.6	16
186	The effect of annealing atmosphere on photoluminescent properties of SiCN films. Surface and Coatings Technology, 2007, 201, 5404-5407.	2.2	16
187	Pure gold nanocages by galvanic replacement reaction of magnesium nanoparticles. RSC Advances, 2014, 4, 1185-1188.	1.7	16
188	Carbon onion growth enhanced by nitrogen incorporation. Scripta Materialia, 2006, 54, 1739-1743.	2.6	15
189	Preparation of semiconductor nanospheres by laser-induced phase separation. Journal of Applied Physics, 2009, 106, 114318.	1.1	15
190	Control of the Morphology and Optical Properties of ZnO Nanostructures via Hot Mixing of Reverse Micelles. Langmuir, 2010, 26, 13755-13759.	1.6	15
191	Facile synthesis of zinc hydroxide carbonate flowers on zinc oxide nanorods with attractive luminescent and optochemical performance. Nanotechnology, 2011, 22, 245607.	1.3	15
192	The effect of low-energy-ion irradiation on photoluminescence of porous silicon. Journal of Applied Physics, 2007, 101, 026101.	1.1	14
193	Magnetic properties and charge ordering in Pr0.75Na0.25MnO3 manganite. Solid State Communications, 2005, 135, 356-360.	0.9	13
194	First-principles study of the B- or N-doping effects on chemical bonding characteristics between magnesium and single-walled carbon nanotubes. Chemical Physics Letters, 2009, 469, 145-148.	1.2	13
195	Effect of annealing on the structure of carbon onions and the annealed carbon coated Ni nanoparticles fabricated by chemical vapor deposition. Journal of Alloys and Compounds, 2009, 472, 230-233.	2.8	13
196	Surface State Induced Ferromagnetism in Co- and Mn-Doped ZnO Surfaces. Journal of Physical Chemistry C, 2011, 115, 3368-3371.	1.5	13
197	Performance comparison of dye-sensitized solar cells with different ZnO photoanodes. Semiconductor Science and Technology, 2011, 26, 105001.	1.0	13
198	Three-dimensional networks of ITO/CdS coaxial nanofibers for photovoltaic applications. Journal of Materials Chemistry, 2012, 22, 13057.	6.7	13

#	Article	IF	CITATIONS
199	Graphene Hybrids: Identifying the Key Role of Pyridinicâ€N–Co Bonding in Synergistic Electrocatalysis for Reversible ORR/OER (Adv. Mater. 23/2018). Advanced Materials, 2018, 30, 1870164.	11.1	13
200	Surface Characterization of Li-Substituted Compositionally Heterogeneous NaLi <sub>0.045</sub> Cu <sub>0.185</sub> Fe <sub>0.265</sub> Mn <sub>0.505</sub> O <sub>2</sub> Sodium-Ion Cathode Material. Journal of Physical Chemistry C, 2019, 123, 11428-11435.	1.5	13
201	Ultrathin cadmium sulfide nanosheets for visible-light photocatalytic hydrogen production. Journal of Materials Chemistry A, 2020, 8, 3586-3589.	5.2	13
202	The properties of granular activated carbons prepared from fly ash using different methods. Carbon, 2006, 44, 1346-1348.	5.4	12
203	Improvement of photoluminescence properties of porous silicon by silica passivation. Applied Surface Science, 2006, 252, 4161-4166.	3.1	12
204	Catalytic synthesis of carbon nanostructures using Fe(OH)3/Al as catalyst precursors. Journal of Alloys and Compounds, 2009, 468, 64-68.	2.8	12
205	Low-temperature synthesis of multi-walled carbon nanotubes over Cu catalyst. Materials Letters, 2012, 72, 164-167.	1.3	12
206	Carbon Nanotube Reinforced CdSe Inverse Opal with Crackâ€Free Structure and High Conductivity for Photovoltaic Applications. Advanced Materials Interfaces, 2015, 2, 1400464.	1.9	12
207	Extraordinary Hall effect and universal scaling in Fe <i>x</i> (ZnO)1– <i>x</i> granular thin films at room temperature. Applied Physics Letters, 2015, 106, .	1.5	12
208	Photothermal synthesis of ultrafine Cu <sub>x</sub> O nanoparticles on carbon nanotubes for photosensitized degradation. Chemical Communications, 2015, 51, 5660-5663.	2.2	12
209	The influence of Si alloying on the crept microstructure and property of a TiAl alloy prepared by powder metallurgy. Intermetallics, 2001, 9, 745-753.	1.8	11
210	Mechanical Properties of Nylon6 Cord-Rubber Composite Subjected to Biaxial Tensile Loads. Journal of Elastomers and Plastics, 2002, 34, 265-278.	0.7	11
211	TEM studies of the initial stage growth and morphologies of bamboo-shaped carbon nanotubes synthesized by CVD. Journal of Alloys and Compounds, 2007, 433, 79-83.	2.8	11
212	Low temperature fabrication of hollow carbon nanospheres over Ni/Al2O3 by the catalytic method. Journal of Alloys and Compounds, 2008, 465, 387-390.	2.8	11
213	Growth dynamics of nanodiamonds synthesized by pulsed-laser ablation. Journal of Applied Physics, 2008, 104, 096102.	1.1	11
214	Gain High-Quality Colloidal Quantum Dots Directly from Natural Minerals. Langmuir, 2015, 31, 2251-2255.	1.6	11
215	Bond-Energy-Integrated Coordination Number: An Accurate Descriptor for Transition-Metal Catalysts. Journal of Physical Chemistry C, 2019, 123, 28248-28254.	1.5	11
216	Properties and microstructure of VC/Cr3C2-doped WC/Co cemented carbides. Rare Metals, 2007, 26, 584-590.	3.6	10

#	Article	IF	CITATIONS
217	The effect of catalyst evolution at various temperatures on carbon nanostructures formed by chemical vapor deposition. Journal of Materials Science, 2009, 44, 2471-2476.	1.7	10
218	Si enhances the growth of B4C nanowires. Journal of Crystal Growth, 2009, 311, 3721-3725.	0.7	10
219	CdTe nanoflake arrays on a conductive substrate: template synthesis and photoresponse property. Journal of Materials Chemistry A, 2014, 2, 957-961.	5.2	10
220	Gas-phase anion exchange towards ZnO/ZnSe heterostructures with intensive visible light emission. Journal of Materials Chemistry C, 2014, 2, 2793-2798.	2.7	10
221	Interface-dominated galvanic replacement reactions in the Zn/Cu <sup>2+</sup> system. Nanotechnology, 2012, 23, 365601.	1.3	9
222	A Rational Design of Heterojunction Photocatalyst CdS Interfacing with One Cycle of ALD Oxide. Journal of Materials Science and Technology, 2016, 32, 489-495.	5.6	9
223	Scalable synthesis of cubic Cu <sub>1.4</sub> S nanoparticles with long-term stability by laser ablation of salt powder. Chemical Communications, 2016, 52, 811-814.	2.2	9
224	Laserâ€Induced Pyridinicâ€Nitrogenâ€Rich Defective Carbon Nanotubes for Efficient Oxygen Electrocatalysis. ChemCatChem, 2019, 11, 6131-6138.	1.8	9
225	Epitaxial Growth of Highâ€Energy Copper Facets for Promoting Hydrogen Evolution Reaction. Small, 2022, 18, e2107481.	5.2	9
226	Sulfateâ€Enabled Nitrate Synthesis from Nitrogen Electrooxidation on a Rhodium Electrocatalyst. Angewandte Chemie, 2022, 134, .	1.6	9
227	Fatigue Properties of Steel Cord-Rubber Composite. Journal of Elastomers and Plastics, 2001, 33, 283-296.	0.7	8
228	Synthesis of carbon nanohorns by the simple catalytic method. Journal of Alloys and Compounds, 2009, 473, 288-292.	2.8	8
229	Strong green emission from ZnSe–Ag2Se nanocomposites. Journal of Alloys and Compounds, 2010, 492, 638-641.	2.8	8
230	Photochemical Synthesis of Ultrafine Cubic Boron Nitride Nanoparticles under Ambient Conditions. Angewandte Chemie, 2015, 127, 7157-7160.	1.6	8
231	In situ synthesis of highly-active Pt nanoclusters via thermal decomposition for high-temperature catalytic reactions. RSC Advances, 2016, 6, 49777-49781.	1.7	8
232	Strong blue emission from zinc hydroxide carbonate nanosheets. Journal of Luminescence, 2016, 177, 242-248.	1.5	8
233	Real time imaging of two-dimensional iron oxide spherulite nanostructure formation. Nano Research, 2019, 12, 2889-2893.	5.8	8
234	A Bond-Energy-Integrated-Based Descriptor for High-Throughput Screening of Transition Metal Catalysts. Journal of Physical Chemistry C, 2020, 124, 5241-5247.	1.5	8

#	Article	IF	CITATIONS
235	Oxidized single nickel atoms embedded in Ru matrix for highly efficient hydrogen evolution reaction. Journal of Alloys and Compounds, 2021, 874, 159909.	2.8	8
236	Segregation of alloying elements in a fully lamellar TiAl alloy. Scripta Materialia, 2001, 45, 19-24.	2.6	7
237	Preparation and annealing effect on photoluminescent properties of Si/SiC thin films by alternate sputtering. Surface and Coatings Technology, 2007, 201, 5408-5411.	2.2	7
238	Silicon Nanodisks via a Chemical Route. Chemistry of Materials, 2008, 20, 3892-3896.	3.2	7
239	Surfactant-assisted synthesis of ZnO–Au nanostructure with good dispersibility. Journal of Alloys and Compounds, 2009, 477, 661-664.	2.8	7
240	Modify the morphology of colloidal Ag2Se nanostructures by laser irradiation. CrystEngComm, 2013, 15, 1685.	1.3	7
241	Formation of Alumina Nanocapsules by High-Energy-Electron Irradiation of Na-dawsonite Nanorods. Scientific Reports, 2013, 3, 3218.	1.6	7
242	Laser-activated gold catalysts for liquid-phase growth of cadmium selenide nanowires. Chemical Communications, 2015, 51, 2145-2148.	2.2	7
243	Laser-driven absorption/desorption of catalysts for producing nanowire arrays in solution. Journal of Materials Chemistry A, 2016, 4, 379-383.	5.2	7
244	Highly Conjugated Graphitic Carbon Nitride Nanofoam for Photocatalytic Hydrogen Evolution. Langmuir, 2022, 38, 1471-1478.	1.6	7
245	Fabrication of short and straight carbon nanotubes by chemical vapor deposition. Materials Science & Engineering A: Structural Materials: Properties, Microstructure and Processing, 2008, 476, 230-233.	2.6	6
246	Kinetics controlled growth of quasi-spherical ZnO single crystal in homogeneous solutions. Journal of Alloys and Compounds, 2008, 461, 527-531.	2.8	6
247	ZnO–Au hybrid nanocrystals via a high temperature reflux route. Materials Letters, 2009, 63, 1093-1095.	1.3	6
248	From nanoparticle chains to nanorods: control of ZnO nanostructures by laser ablation. Semiconductor Science and Technology, 2011, 26, 075001.	1.0	6
249	Electrodeposition of Silver Nanoparticles on ITO Films with Different Thickness and Application as LSPR Sensor. ECS Electrochemistry Letters, 2014, 3, B30-B32.	1.9	6
250	CdO nanoflake arrays on ZnO nanorod arrays for efficient detection of diethyl ether. RSC Advances, 2016, 6, 2500-2503.	1.7	6
251	Tuning Band Structure of Cadmium Chalcogenide Nanoflake Arrays via Alloying for Efficient Photoelectrochemical Hydrogen Evolution. Langmuir, 2017, 33, 6457-6463.	1.6	6
252	Synthesis of cadmium chalcogenides nanowires via laser-activated gold catalysts in solution. Materials Chemistry and Physics, 2018, 212, 408-414.	2.0	6

#	Article	IF	CITATIONS
253	Laser Synthesized Bi-functional Hybrid Catalyst Oxygen-defective Co <sub>3</sub> O <sub>4â^'x</sub> /N-Graphene for Oxygen Electrode Reactions. Chemistry Letters, 2019, 48, 118-121.	0.7	6
254	Electroreduction of Carbon Dioxide in Metallic Nanopores through a Pincer Mechanism. Angewandte Chemie, 2020, 132, 19459-19465.	1.6	6
255	Distribution of alkali cations near the Cu (111) surface in aqueous solution. Journal of Materials Chemistry A, 2020, 8, 24428-24437.	5.2	6
256	A Hydrogenâ€Deficient Nickel–Cobalt Double Hydroxide for Photocatalytic Overall Water Splitting. Angewandte Chemie, 2020, 132, 11607-11612.	1.6	6
257	Metal-Confined Synthesis of ZnS <sub>2</sub> Monolayer Catalysts for Dinitrogen Electroreduction. ACS Catalysis, 2022, 12, 6809-6815.	5.5	6
258	The enhancement of photoluminescence from porous silicon with Si–Ti bond. Materials Letters, 2005, 59, 3135-3137.	1.3	5
259	Microporous silicon connected with silicon wires. Semiconductor Science and Technology, 2006, 21, 498-500.	1.0	5
260	Synthesis of Si–C nanostructures by laser ablation of silicon target in n-heptane vapor. Materials Letters, 2009, 63, 2492-2494.	1.3	5
261	The production of carbon-microtube rings by a template mechanism. Carbon, 2009, 47, 1877-1880.	5.4	5
262	Synergistic synthesis of quasi-monocrystal CdS nanoboxes with high-energy facets. Journal of Materials Chemistry A, 2015, 3, 23106-23112.	5.2	5
263	Exposing Cu(100) Surface via Ion-Implantation-Induced Oxidization and Etching for Promoting Hydrogen Evolution Reaction. Langmuir, 2022, 38, 2993-2999.	1.6	5
264	Self-supporting copper electrode prepared by ultrasonic impact for hydrogen evolution reaction. Journal of Alloys and Compounds, 2022, 916, 165283.	2.8	5
265	Intrinsic ultraviolet light-emission from Si nanocrystals prepared by reactive sputtering. Journal of Applied Physics, 2006, 100, 076102.	1.1	4
266	The Synthesis of Carbon Nanotubes by Pulsed-Laser Ablation of a Nickel/Carbon Composite Target in Ethanol or Ambient Air. Science of Advanced Materials, 2012, 4, 463-466.	0.1	4
267	A silver catalyst with a high-energy surface prepared by plasma spraying for the hydrogen evolution reaction. Chemical Communications, 2022, 58, 2878-2881.	2.2	4
268	Polycrystalline CoOâ^'Co <sub>9</sub> S <sub>8</sub> Heterostructure Nanoneedle Arrays as Bifunctional Catalysts for Efficient Overall Water Splitting. ChemElectroChem, 2022, 9, .	1.7	4
269	Mechanically processing copper plate into active catalyst for electrochemical hydrogen production. Acta Materialia, 2022, 237, 118164.	3.8	4
270	High-density SiC nanocrystals with strong photoluminescence via a nitrogen-loss route. Semiconductor Science and Technology, 2008, 23, 035015.	1.0	3

#	Article	IF	CITATIONS
271	Synthesis of Carbon Encapsulated Nickel Nanoparticles by Laser Ablation in Liquid. Applied Mechanics and Materials, 0, 110-116, 5487-5494.	0.2	3
272	Engineering hollow electrodes for hybrid solar cells for efficient light harvesting and carrier collection. Journal of Materials Chemistry A, 2016, 4, 17260-17266.	5.2	3
273	Plasmonic Materials: 3D Aluminum Hybrid Plasmonic Nanostructures with Large Areas of Dense Hot Spots and Longâ€Term Stability (Adv. Funct. Mater. 10/2017). Advanced Functional Materials, 2017, 27, .	7.8	3
274	Fine regulation of electron transfer in Ag@Co <sub>3</sub> O <sub>4</sub> nanoparticles for boosting the oxygen evolution reaction. Chemical Communications, 2021, 57, 6284-6287.	2.2	3
275	Regulating the work function of silver catalysts <i>via</i> surface engineering for enhanced CO <sub>2</sub> electroreduction. Physical Chemistry Chemical Physics, 2022, , .	1.3	3
276	γ ↔ α2 Phase transformation in fractured high temperature stress rupture Ti-48Al-2Nb(at.%). Journal of Materials Science, 2000, 35, 4501-4505.	1.7	2
277	Creepâ€induced phase transformations in a Ti-Al alloy. Philosophical Magazine A: Physics of Condensed Matter, Structure, Defects and Mechanical Properties, 2002, 82, 39-50.	0.7	2
278	Hybrid nanocomposite of Fe nanoparticles on SiO2 nanowires by sublimation route. Materials Letters, 2007, 61, 3783-3786.	1.3	2
279	Structure and photoluminescence of SiC/ZnO nanocomposites prepared by radio frequency alternate sputtering. Journal of Materials Science, 2010, 45, 6657-6660.	1.7	2
280	Decolorization of methylene blue in aqueous suspensions of gold nanoparticles using parallel nanosecond pulsed laser. Journal of Environmental Science and Health - Part A Toxic/Hazardous Substances and Environmental Engineering, 2013, 48, 1583-1591.	0.9	2
281	One Step Growth of Semiconductor CdS Uniform Branched Nanowire on FTO. Applied Mechanics and Materials, 0, 472, 744-749.	0.2	2
282	Hierarchical, Ultrathin Single-Crystal Nanowires of CdS Conveniently Produced in Laser-Induced Thermal Field. Langmuir, 2015, 31, 8162-8167.	1.6	2
283	Electrocatalysis: Wellâ€Dispersed Nickel―and Zincâ€Tailored Electronic Structure of a Transition Metal Oxide for Highly Active Alkaline Hydrogen Evolution Reaction (Adv. Mater. 16/2019). Advanced Materials, 2019, 31, 1970113.	11.1	2
284	Blue-light emission from porous silicon induced by laser irradiation. Materials Letters, 2005, 59, 2394-2397.	1.3	1
285	Preferential growth of Si nanocrystals in SiO2/Si/SiO2 sandwich structure. Journal of Crystal Growth, 2007, 305, 59-62.	0.7	1
286	Preparation of 3YSZ/Cu composite by in-situ chemical route. Journal of Materials Science, 2007, 42, 5671-5675.	1.7	1
287	TiO2 cellular-protected nanowire array fabricated super-rapidly by the precipitation of colloids in the nanopores. Journal of Materials Chemistry, 2012, 22, 13820.	6.7	1
288	ZnSe hollow nanospheres in mechanically stable near-IR antireflection coatings for ZnSe substrates. Nanotechnology, 2016, 27, 365604.	1.3	1

#	Article	IF	CITATIONS
289	Microwave activated gold nanoparticles for catalytic growth of monocrystal CdSe nanowires in solution. New Journal of Chemistry, 2017, 41, 14822-14825.	1.4	1
290	Near-infrared graded-index antireflection coating from ZnSe hollow nanospheres. Materials Letters, 2018, 222, 21-24.	1.3	1
291	Spheroidization of Nickel Powder and Coating with Carbon Layer through Laser Heating. Materials, 2018, 11, 1641.	1.3	1
292	Ultra-fine Nanodiamonds Synthesized Using Millisecond-pulsed Laser. Wuli Huaxue Xuebao/ Acta Physico - Chimica Sinica, 2007, 23, 1105-1108.	2.2	1
293	The effect of sputtering deposition rate on the agglomeration and crystallization of Si clusters. Materials Letters, 2007, 61, 4079-4082.	1.3	0
294	Fabrication and Growth Mechanism of Carbon Nanotubes by Chemical Vapor Deposition. Journal of Computational and Theoretical Nanoscience, 2008, 5, 1464-1469.	0.4	0
295	CdS Quantum Dots Sensitized One-Dimensional ZnO Solar Cells with Improved Efficiency Using ZnS Shell Coating. , 2010, , .		0
296	Photocatalytic Degradation of 2,4,5–TCP in TiO <sub>2</sub> /UV/H <sub>2</sub> O <sub>2</sub> System. Advanced Materials Research, 2012, 518-523, 2649-2652.	0.3	0
297	Nanoflake Arrays: CdS Nanoflake Arrays for Highly Efficient Light Trapping (Adv. Mater. 4/2015). Advanced Materials, 2015, 27, 772-772.	11.1	0
298	Water Splitting: Strongly Coupled Nafion Molecules and Ordered Porous CdS Networks for Enhanced Visible-Light Photoelectrochemical Hydrogen Evolution (Adv. Mater. 24/2016). Advanced Materials, 2016, 28, 4943-4943.	11.1	0
299	Functional nanostructures obtained by laser ablation. , 2012, , .		Ο